CHEMISTRY OF MATERIALS

ARTICLE

pubs.acs.org/cm

Synthesis and Photovoltaic Properties of D−A Copolymers Based on Alkyl-Substituted Indacenodithiophene Donor Unit

Maojie Zhang,[†,§] Xia Guo,[†,§] Xiaochen Wang,[‡] Haiqiao Wang,[‡] and Yongfang Li*[,†]

[†]Beijing National Laboratory for Molecular Sciences, CAS Key Laboratory of Organic Solids, Institute of Chemistry, Chinese Academy of Sciences, Beijing 100190, China

[‡]Key Laboratory of Advanced Process and Preparation Technique of Nanomaterials, Ministry of Education, College of Materials Science and Engineering, Beijing University of Chemical Technology, Beijing 100029, China

[§]Graduate University of Chinese Academy of Sciences, Beijing 100049, China

ABSTRACT:

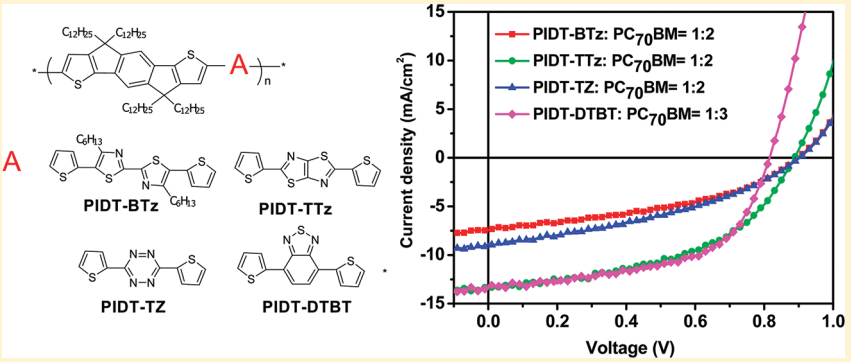

Four D−A copolymers of tetradodecyl-substituted indacenodithiophene (IDT) donor unit with different acceptor units including bis(thiophen-2-yl)-bithiazole (BTz), bis(thiophen-2-yl)thiazolothiazole (TTz), bis(thiophen-2-yl)-tetrazine (TZ), and bis-(thiophen-2-yl)-benzothiadiazole (DTBT), **PIDT-BTz**, **PIDT-TTz**, **PIDT-TZ**, and **PIDT-DTBT**, were synthesized for the application as donor materials in polymer solar cells (PSCs). The copolymers possess good solubility benefitted from the four alkyl side chains on IDT unit, deeper HOMO levels at ca. −5.2 eV thanks to the IDT unit and tunable bandgap depending on the acceptor units. Among the copolymers, **PIDT-TTz** has the highest hole mobility (μ_h) of 4.99 × 10^{-3} cm^2/V s. The power conversion efficiency (PCE) of the PSC based on **PIDT-TTz**/$PC_{70}BM$ (1:2 w/w) reached 5.79%, under the illumination of AM1.5G, 100 mW/cm^2. **PIDT-DTBT** film has the smallest bandgap of 1.68 eV and a higher μ_h of 2.24 × 10^{-3} cm^2/V s. The PSC based on **PIDT-DTBT**/$PC_{70}BM$ (1:3 w/w) exhibited an even higher PCE of 6.17% with a J_{sc} of 13.27 mA/cm^2, a V_{oc} of 0.82 V, and a FF of 56.9%.

KEYWORDS: polymer solar cell, conjugated D−A copolymers, indacenodithiophene, bandgap, power conversion efficiency

INTRODUCTION

In the past decade, bulk heterojunction (BHJ) polymer solar cells (PSCs) have attracted considerable attention for applications in renewable energy due to their advantages of having low cost and easy fabrication, being lightweight, and having the capability to fabricate flexible large-area devices.[1−5] The key component of the PSCs is the photoactive layer composed of a blend of a conjugated polymer donor and a fullerene derivative acceptor (such as [6,6]-phenyl-C_{61}-butyric acid methyl ester ($PC_{60}BM$) or [6,6]-phenyl-C_{71}-butyric acid methyl ester ($PC_{70}BM$)). For increasing power conversion efficiency (PCE) of the PSCs, great efforts have been devoted to the design and synthesis of new conjugated polymer donor[2−16] and new fullerene derivative acceptor[17] photovoltaic materials.

High efficiency conjugated polymer donor materials need to possess broad absorption in visible and near-infrared region (narrower bandgap), higher hole mobility, and relatively lower-lying HOMO (the highest occupied molecular orbital) energy levels.[2−5] To date, the design and synthesis of donor−acceptor (D−A) copolymers has been proven to be one of the most successful strategies to satisfy the above requirements.[8−16] This D−A approach for designing the polymers is highly effective for tuning band gap, energy levels, and charge carrier mobility by choosing a suitable combination from the vast variety of donor units and acceptor units available.[18] Recently, significant progress has been made in new D−A copolymers to enable PSC devices to show high PCEs (>7%).[15,16]

Among various donor units, indacenodithiophene (IDT) has attracted much interest in the design of new conjugated copolymers for the application in optoelectronic devices.[19−21] The coplanarity of the IDT unit could enhance interchain interaction of the polymers and expect to have higher hole mobility.[22] Chen

Received: July 9, 2011
Revised: August 21, 2011
Published: September 02, 2011

Scheme 1. Synthetic Route of the D−A Copolymers

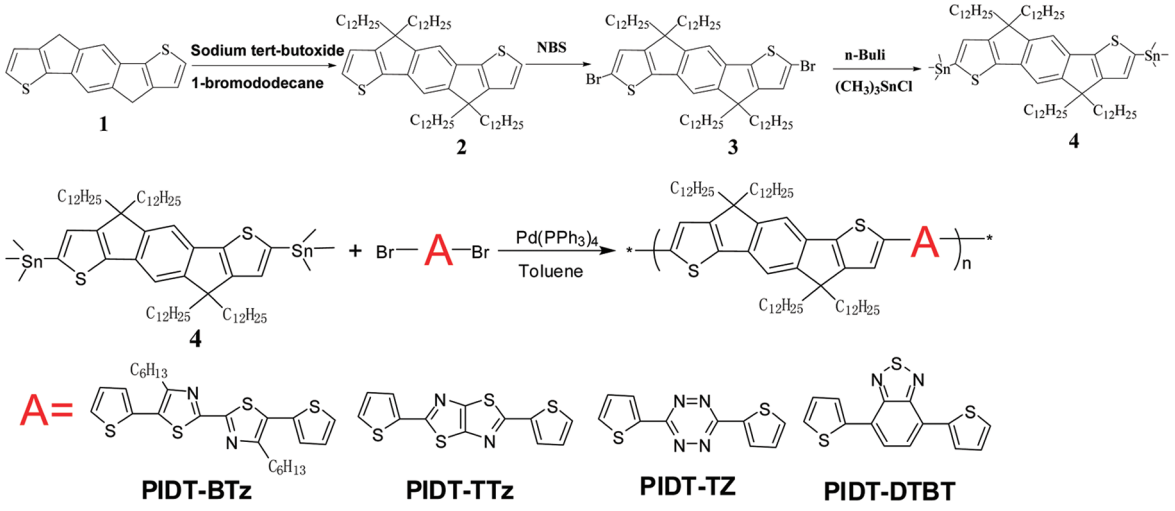

Table 1. Molecular Weights and Thermal Properties of the Copolymers

polymers	M_w[a]	M_n[a]	PDI[a]	T_d (°C)[b]
PIDT-BT$_Z$	24.9 K	13.6 K	1.83	271
PIDT-TT$_Z$	27.6 K	17.4 K	1.59	334
PIDT-TZ	13.3 K	8.7 K	1.53	278
PIDT-DTBT	21.3 K	11.7 K	1.82	406

[a] M_n, M_w, and PDI of the polymers were determined by GPC using polystyrene standards in THF. [b] The 5% weight-loss temperatures under inert atmosphere.

et al.[19] and Jen et al.[20] synthesized a series of copolymers based on IDT with aryl substituent, which showed a field effect hole mobility up to ~10^{-2} cm^2/V s and high PCE of ~6%.[19,20] Recently, Zhang et al. reported copolymers based on IDT with alkyl substituent which showed a high field effect hole mobility of up to 1 cm^2/V s.[21] However, to the best of our knowledge, there is no work on the copolymers based on the IDT unit with alkyl substituent for the photovoltaic applications. In comparison with the IDT unit with aryl side chains, the IDT unit with alkyl side chains should possesses better solubility. Considering the good planarity of the IDT unit, good solubility, the high hole mobility of the copolymers based on the IDT unit with alkyl substituents, and the promising photovoltaic properties of the D−A copolymers, in this work, we synthesized a new derivative of alkyl-substituted indacenodithiophene (IDT) and used it as a donor unit for D−A copolymers. Here, we synthesized four IDT-based copolymers **PIDT-BTz**, **PIDT-TTz**, **PIDT-TZ**, and **PIDT-DTBT**(see Scheme 1) with different acceptor building blocks including bis(thiophen-2-yl)-bithiazole (BTz), bis(thiophen-2-yl)-thiazolothiazole (TTz), bis(thiophen-2-yl)-tetrazine (TZ), or bis(thiophen-2-yl)-benzothiadiazole (DTBT) to tune the absorption and molecular energy levels to meet the requirements of high efficiency conjugated polymer donor materials. The copolymers possess good solubility in common organic solvents, deeper HOMO energy level at ca. −5.2 eV, and tunable bandgap, depending on the acceptor units. Among the copolymers, **PIDT-TTz** has high hole mobility (μ_h) of 4.99×10^{-3} cm^2/V s. PCE of the PSC based on **PIDT-TTz**/$PC_{70}BM$ (1:2 w/w) reached 5.79%, under the illumination of AM1.5G, 100 mW/cm^2. **PIDT-DTBT** film has a bandgap of 1.68 eV and a higher μ_h of 2.24×10^{-3} cm^2/V s. The PSC based on **PIDT-DTBT**/$PC_{70}BM$ (1:3 w/w) exhibited an even higher PCE of 6.17%. These results indicate that the D−A copolymers based on the alkyl-substituted IDT donor unit are promising photovolaic polymer donor materials for high efficiency PSCs.

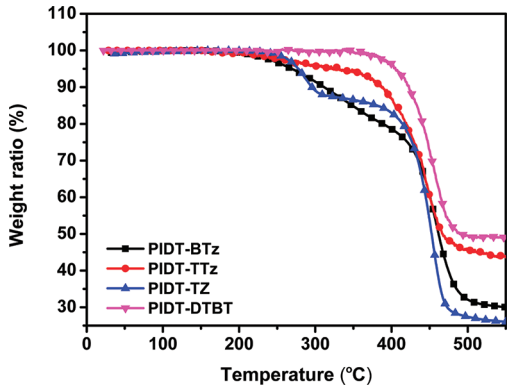

Figure 1. TGA plots of the copolymers with a heating rate of 10 °C min^{-1} under inert atmosphere.

RESULTS AND DISCUSSION

Synthesis and Thermal Stability. The general synthetic strategy for monomer **4** and the copolymers is outlined in Scheme 1. The four copolymers were synthesized by the Pd-catalyzed Stille-coupling reaction. The polymers all show good solubility at room temperature in common organic solvents such as chloroform ($CHCl_3$), tetrahydrofuran (THF), toluene, and chlorobenzene. The weight-average molecular weight (M_w) and polydispersity index (PDI) were measured by gel permeation chromatography (GPC) using THF as the eluent and polystyrenes as the internal standards, and the results were listed in Table 1. The M_w of **PIDT-BT$_Z$**, **PIDT-TT$_Z$**, **PIDT-TZ**, and **PIDT-DTBT** are 24.9 K, 27.6 K, 13.3 K, and 21.3 K, respectively. Molecular weights of the copolymers are relatively low, due probably to low purity of

dx.doi.org/10.1021/cm2019586 |Chem. Mater. 2011, 23, 4264–4270

monomer **4** in the copolymerization. Monomer **4** is difficult to be purified by the common purification methods such as recrystallization or column chromatography.

Thermal stability of the polymers was investigated with thermogravimetric analysis (TGA), as shown in Figure 1. The TGA analysis reveals that the onset temperatures with 5% weight-loss (T_d) of **PIDT-BTz**, **PIDT-TTz**, **PIDT-TZ**, and **PIDT-DTBT** are 271, 334, 278, and 406 °C, respectively. This indicates that the thermal stability of the copolymers is good enough for the applications in PSCs.

Optical Properties. Figure 2 shows the ultraviolet−visible (UV−vis) absorption spectra of the polymer dilute solutions in chloroform and films spin-coated on quartz substrates. The detailed absorption data, including absorption maximum wavelength of solutions and films, the absorption edge (onset wavelength of the absorption peak, λ_{onset}) of the polymer films, and the optical bandgap deduced from the absorption edges, are summarized in Table 2. In Figure 2a, the absorption maxima of the polymer solutions are 508, 587, 584, and 605 nm for **PIDT-BTz**, **PIDT-TTz**, **PIDT-TZ**, and **PIDT-DTBT**, respectively. **PIDT-BTz** exhibits the absorption maximum at a relatively short wavelength, which might be ascribed to a relatively weak acceptor unit of BTz. In addition, too much side chains on the polymer could cause a steric interaction between the alkyl chains which results in twisting of the polymer main chain. **PIDT-TTz** and **PIDT-TZ** show similar absorption spectra which are red-shifted by ca. 80 nm in comparison with that of **PIDT-BTz**. **PIDT-DTBT** displays the broadest absorption with absorption edge extending to ca. 720 nm. In addition, the absorption spectrum of **PIDT-DTBT** shows two peaks, a typical feature for the D−A copolymers. The absorption peak around 430 nm could be originated from the $\pi-\pi^*$ transition of the polymer main chain, while the absorption peak around 605 nm should be attributed to the strong ICT (intermolecular charge transfer) interaction between IDT donor unit and DTBT acceptor unit. The absorption spectra of the polymer films, as shown in Figure 2b, are all red-shifted and broadened in comparison with those of their solutions, which is a common phenomenon for the conjugated polymers, owing to the aggregation of the conjugated polymer main chains in the solid films. The absorption edges (λ_{edge}) of the four polymer films are 620, 675, 680, and 735 nm for **PIDT-BTz**, **PIDT-TTz**, **PIDT-TZ**, and **PIDT-DTBT**, respectively, from which the optical bandgaps (E_g^{opt}) of the polymers were calculated according to $E_g^{opt} = 1240/\lambda_{edge}$ and the results were listed

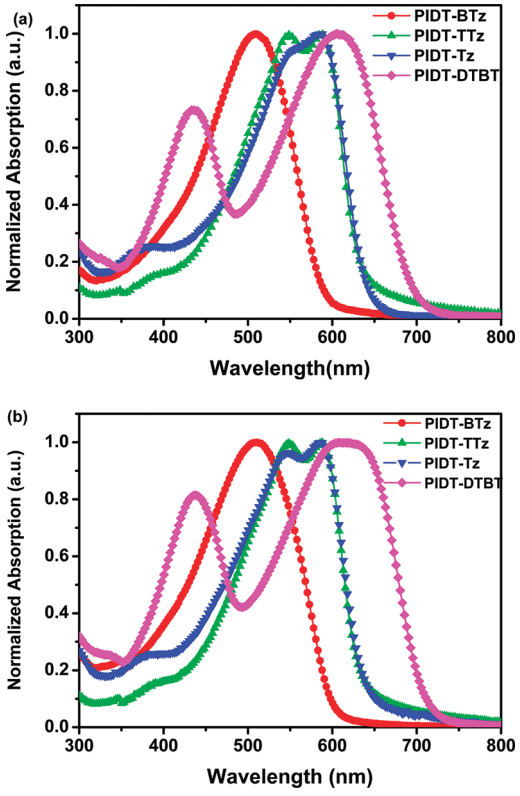

Figure 2. Absorption spectra of the copolymers (a) in chloroform solutions and (b) in solid films.

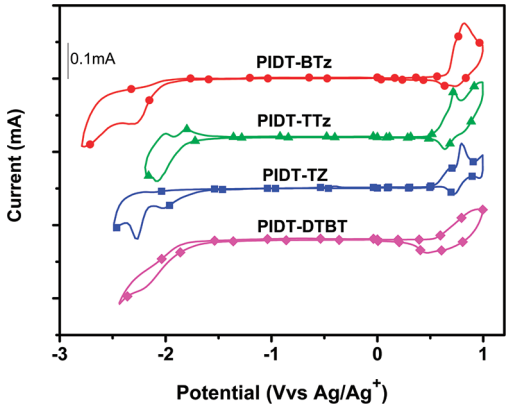

Figure 3. Cyclic voltammograms of the copolymer films on a platinum electrode measured in 0.1 mol/L Bu_4NPF_6 acetonitrile solutions at a scan rate of 100 mV/s.

Table 2. Optical and Electrochemical Properties of the Polymers

	UV−vis absorption spectra				cyclic voltammetry		
	solution[a]	film[b]			p-doping	n-doping	
polymers	λ_{max} (nm)	λ_{max} (nm)	λ_{onset} (nm)	E_g^{optc} (eV)	φ_{ox}/HOMO (V)/(eV)	φ_{red}/LUMO (V)/(eV)	E_g^{EC} (eV)
PIDT-BTz	508	510	620	2.0	0.55/−5.26	−1.91/−2.80	2.46
PIDT-TTz	587	590	675	1.83	0.50/−5.21	−1.77/−2.94	2.27
PIDT-TZ	584	585	680	1.82	0.51/−5.22	−1.74/−2.97	2.25
PIDT-DTBT	605	615	735	1.68	0.53/−5.24	−1.61/−3.10	2.14

[a] Measured in chloroform solution. [b] Cast from chloroform solution. [c] Bandgap estimated from the onset wavelength (λ_{edge}) of the optical absorption: $E_g^{opt} = 1240/\lambda_{edge}$.

dx.doi.org/10.1021/cm2019586 |*Chem. Mater.* 2011, 23, 4264–4270

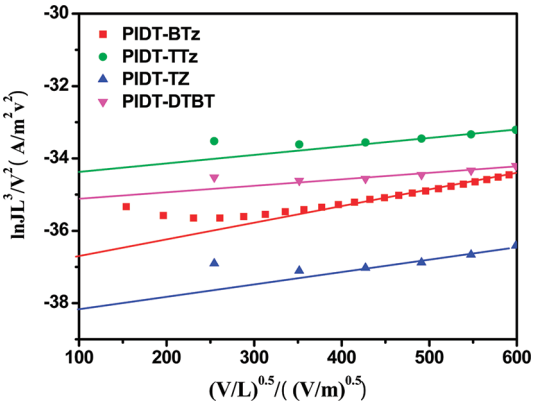

Figure 4. $\ln(JL^3/V^2)$ versus $(V/L)^{0.5}$ plots for the measurement of the hole mobility of the copolymers by the SCLC method.

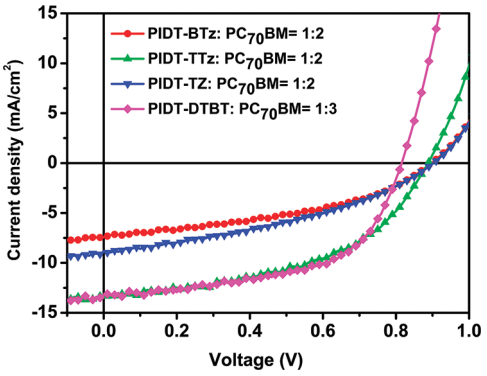

Figure 5. $J-V$ curves of the PSCs based on polymers/$PC_{70}BM$ under the illumination of AM 1.5, 100 mW/cm^2.

in Table 2. With the increase of the electron-withdrawing ability of the acceptor unit from BTz to TTz, TZ, and DTBT, the bandgap of the corresponding D−A copolymers shifted from 2.0 to 1.83, 1.82, and 1.68 eV, respectively. The smaller bandgap and broad absorption of **PIDT-DTBT** should be beneficial to its application as photovoltaic material in PSCs.

Electrochemical Properties. The electrochemical cyclic voltammetry was performed for determining the highest occupied molecular orbital (HOMO) and the lowest unoccupied molecular orbital (LUMO) energy levels of the conjugated polymers.[23] Figure 3 shows the cyclic voltammograms (CVs) of the copolymer films on Pt disk electrode in 0.1 mol/L Bu_4NPF_6 acetonitrile solution. The onset reduction potentials (φ_{red}) of **PIDT-BTz**, **PIDT-TTz**, **PIDT-TZ**, and **PIDT-DTBT** are −1.91, −1.77, −1.74, and −1.61 V vs. Ag/Ag$^+$, respectively, while the onset oxidation potentials (φ_{ox}) are 0.55, 0.50, 0.51, and 0.53 V vs. Ag/Ag$^+$, respectively.

From φ_{ox} and φ_{red} of the polymers, HOMO and LUMO energy levels as well as the energy gap (E_g^{EC}) of the polymers were calculated according to the equations,[24]

$$\text{HOMO} = -\text{e}(\varphi_{ox} + 4.71)(\text{eV})$$

$$\text{LUMO} = -\text{e}(\varphi_{red} + 4.71)(\text{eV})$$

$$Eg^{EC} = \text{e}(\varphi_{ox} - \varphi_{red})(\text{eV})$$

where the units of φ_{ox} and φ_{red} are V vs Ag/Ag$^+$.

The results of the electrochemical measurements are listed in Table 2. The LUMO energy levels of **PIDT-BTz**, **PIDT-TTz**, **PIDT-TZ**, and **PIDT-DTBT** are −2.80, −2.94, −2.97, and −3.10 eV, respectively. The HOMO energy levels of **PIDT-BTz**, **PIDT-TTz**, **PIDT-TZ**, and **PIDT-DTBT** are −5.26, −5.21, −5.22, and −5.24 eV, respectively. The electrochemical bandgaps are 2.46, 2.27, 2.25, and 2.14 eV for **PIDT-BTz**, **PIDT-TTz**, **PIDT-TZ**, and **PIDT-DTBT**, respectively. The LUMO energy levels of the polymers decreased significantly with the increase of the electron-withdrawing ability of the acceptor unit from BTz to TTz, TZ, and DTBT, but the HOMO energy levels of the polymers change little. All the copolymers have relatively deeper HOMO energy levels of ca. −5.2 eV, which is desirable for higher open circuit voltage (V_{oc}) of the PSCs with the polymers as donor photovoltaic materials, since V_{oc} of PSCs is related to the difference of the LUMO of the electron acceptor and the HOMO of the electron donor.[25]

Table 3. Photovoltaic Performances of the PSCs Based on Polymer/$PC_{70}BM$ under the Illumination of AM1.5, 100 mW/cm^2

polymers	blend ratio with $PC_{70}BM$	V_{oc} (V)	J_{sc} (mA/cm^2)	FF (%)	PCE (%)
PIDT-BTz	1:2	0.90	7.43	41.4	2.77
PIDT-TTz	1:2	0.89	13.3	48.9	5.79
PIDT-TZ	1:2	0.90	8.85	38.1	3.04
PIDT-DTBT	1:3	0.82	13.27	56.7	6.17

Hole Mobility. Hole mobility is another important parameter for the conjugated polymer donor photovoltaic materials. Here, we measured the hole mobilities of the copolymers by the space-charge limit current (SCLC) method using a device structure of ITO/PEDOT−PSS/polymer/Au. For the hole-only devices, SCLC is described by[26]

$$J \cong (9/8)\varepsilon\varepsilon_0\mu_0 V^2 \exp(0.89\sqrt{V/E_0 L})/L^3 \quad (1)$$

where ε is the dielectric constant of the polymer, ε_0 is the permittivity of the vacuum, μ_0 is the zero-field mobility, E_0 is the characteristic field, J is the current density, L is the thickness of the blended films layer, $V = V_{appl} - V_{bi}$, V_{appl} is the applied potential, and V_{bi} is the built-in potential which results from the difference in the work function of the anode and the cathode (in this device structure, V_{bi} = 0.2 V). Figure 4 shows $\ln(JL^3/V^2)$ versus $(V/L)^{0.5}$ plots for the measurement of the hole mobility of the copolymers by the SCLC method. According to eq 1, the hole mobilities obtained are 5.0×10^{-4} cm^2/V s, 4.99×10^{-3} cm^2/V s, 1.11×10^{-4} cm^2/V s, and 2.24×10^{-3} cm^2/V s for **PIDT-BTz**, **PIDT-TTz**, **PIDT-TZ**, and **PIDT-DTBT**, respectively. Obviously, the hole mobilities of PIDT-TTz and PIDT-DTBT are good (higher than 10^{-3} cm^2/V s) for the application as photovoltaic donor materials in PSCs.

Photovoltaic Properties. To investigate and compare the photovoltaic properties of the four copolymers, bulk heterojunction PSC devices with a configuration of ITO/PEDOT:PSS/polymer:$PC_{70}BM$/Ca/Al were fabricated. Figure 5 shows the $I-V$ curves of the PSCs under the illumination of AM1.5, 100 mW/cm^2. The open-circuit voltage (V_{oc}), short-circuit current (J_{sc}), fill factor (FF), and power conversion efficiency (PCE) of the PSCs are summarized in Table 3. The polymer solar cells (PSCs) based on **PIDT-BTz**/, **PIDT-TTz**/, **PIDT-TZ**/, or

dx.doi.org/10.1021/cm2019586 |*Chem. Mater.* 2011, 23, 4264–4270

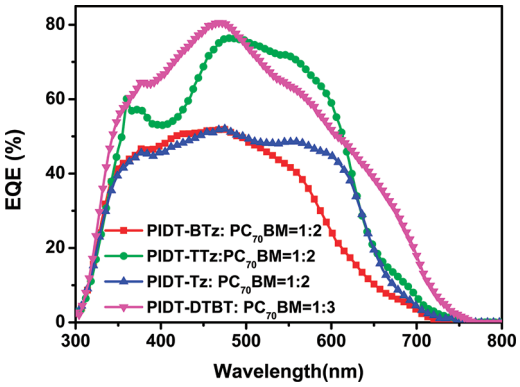

Figure 6. EQE of the PSCs based on the blend of polymers and $PC_{70}BM$.

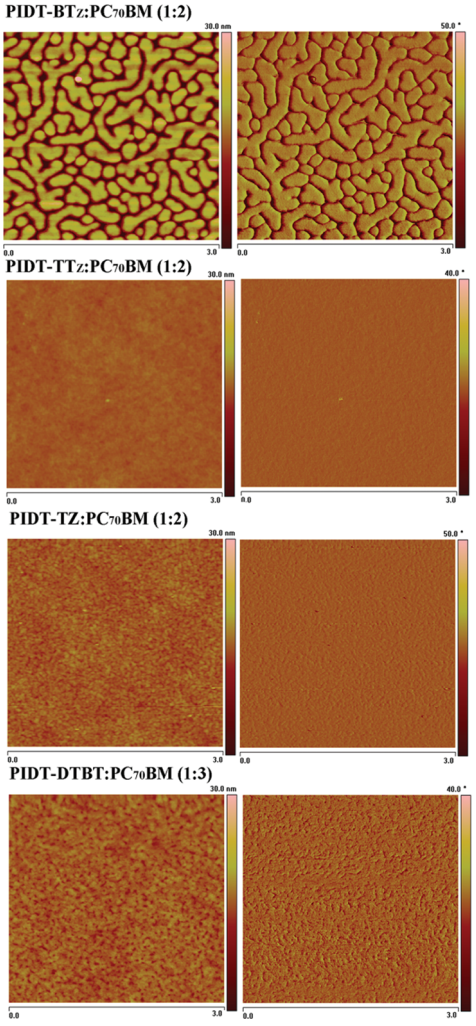

Figure 7. AFM topography (left) and phase (right) images of the blend films of polymer/$PC_{70}BM$, the size of the image is 3 μm × 3 μm.

PIDT-DTBT/$PC_{70}BM$ all exhibited high open circuit voltage (V_{oc}) over 0.8 V, benefited from the deep HOMO energy levels of the polymers. The PSCs based on **PIDT-BTz** and **PIDT-TZ** exihibited lower FF of 41.4% and 38.1%, respectively, which could be caused by their lower hole mobility. The power conversion efficiency (PCE) of the polymer solar cell (PSC) based on **PIDT-TTz**/$PC_{70}BM$ (1:2 w/w) reached 5.79% with a large short circuit current (J_{sc}) of 13.3 mA/cm^2 and a high open circuit voltage (V_{oc}) of 0.89 V and a FF of 48.9%, under the illumination of AM1.5G, 100 mW/cm^2. The good photovoltaic performance of **PIDT-TTz** could be ascribed to its high hole mobility (4.99×10^{-3} cm^2/V s). The PSC based on **PIDT-DTBT**/$PC_{70}BM$ (1:3 w/w) exhibited an even higher PCE of 6.17% with a J_{sc} of 13.27 mA/cm^2, a V_{oc} of 0.82 V, and a FF of 56.7%. The high photovoltaic performance of **PIDT-DTBT** should be benefited from its high hole mobility and broader absorption.

The external quantum efficiencies (EQE) as a function of wavelength of the photovoltaic cells based on **PIDT-BTz**, **PIDT-TTz**, **PIDT-TZ**, or **PIDT-DTBT**/$PC_{70}BM$ blend are shown in Figure 6. The EQE curves of the polymer/$PC_{70}BM$ blend all cover a broad wavelength from 350 to 700 nm and show a maximum EQE value of 52.3% at ~460 nm, 76% at ~480 nm, 52% at ~470 nm, and 81% at ~470 nm for the PSCs based on **PIDT-BTz**, **PIDT-TTz**, **PIDT-TZ**, and **PIDT-DTBT**, respectively. The greater EQE values of the PSCs based on **PIDT-TTz** and **PIDT-DTBT** agree with the high J_{sc} of the corresponding devices. In the wavelength range of 350−500 nm, the high EQE values of the device based on **PIDT-DTBT**/$PC_{70}BM$ should result from both the strong absorption of $PC_{70}BM$ in the active layer of **PIDT-DTBT**/$PC_{70}BM$ with a high $PC_{70}BM$ weight ratio of 1:3 and the absorption peak of **PIDT-DTBT** film in the wavelength range of 350−500 nm (see Figure 2b).

In order to understand the effect of mophology of the photoactive layers on the photovoltaic performance of the polymer solar cells, the mophological structures of the blend films of polymer/$PC_{70}BM$ were analyzed by tapping mode atom force microscopy (AFM) measurements. Figure 7 shows the AFM images of the blend films. The morphological requirement for the active layer in high performance PSCs is nanoscale phase separation, which enables a large interface area for exciton dissociation and, in the mean time, a continuous percolating path for hole and electron transport to the corresponding electrodes.[27] The film of **PIDT-BTz**/$PC_{70}BM$ (1:2, w/w) showed clear phase separation with a large domain size over 100 nm and a high surface roughness of 4−5 nm, which is not good for excition transportation and dissociation on the interface of polymer and $PC_{70}BM$. The blend films based on **PIDT-TTz**, **PIDT-TZ**, and **PIDT-DTBT** all demonstrated low roughness of 0.34, 0.75, and 0.91 nm, respectively. Although with a smooth morphology, the device based on **PIDT-TZ**/$PC_{70}BM$ demonstrated the low FF of 38.1% which should result from the low hole mobility of **PIDT-TZ**. For the **PIDT-TTz**/$PC_{70}BM$ or **PIDT-DTBT**/$PC_{70}BM$ blend film, the bright patterns of polymer domains all showed a good interpenetrating network which is beneficial to the exciton dissociation and charge carriers transport. Obviously, the suitable morphology of the blend films are consistent with the higher photovoltaic performance of the PSCs based on **PIDT-TTz** and **PIDT-DTBT**.

CONCLUSION

We have successfully sythesized four D−A copolymers of tetradodecyl-substituted IDT donor unit and different acceptor units including BTz, TTz, TZ, and DTBT, **PIDT-BTZ**, **PIDT-TTZ**, **PIDT-TZ**, and **PIDT-DTBT**, by the Pd-catalyzed Stille-coupling reaction. Introduction of the alkyl-substituted IDT donor unit leads to good solubility and deeper HOMO energy

level (ca. −5.2 eV) of the copolymers, and the different acceptor units tune the bandgap of the D−A copolymers from 2.0 eV for **PIDT-BTz** to 1.68 eV for **PIDT-DTBT**. The copolymers of IDT with TTz or DTBT also demonstrate high hole mobilities: 4.99×10^{-3} cm^2/V s for **PIDT-TTz** and 2.24×10^{-3} cm^2/V s for **PIDT-DTBT.** The PSCs based on the copolymers as donor all show high V_{oc} of 0.82−0.90 V, which is benefited from the deeper HOMO energy level of the polymers. The PCE of the PSC based on **PIDT-TTz**/$PC_{70}BM$ (1:2 w/w) reached 5.79% with a large J_{sc} of 13.3 mA/cm^2 and a high V_{oc} of 0.89 V, under the illumination of AM1.5G, 100 mW/cm^2. The PSC based on **PIDT-DTBT**/$PC_{70}BM$ (1:3 w/w) exhibited an even higher PCE of 6.17% with a J_{sc} of 13.27 mA/cm^2, a V_{oc} of 0.82 V, and a FF of 56.9%. The results indicate that the D−A copolymers based on the IDT donor unit with alkyl side chains are promising photovoltaic polymer donor materials for high efficiency PSCs.

EXPERIMENTAL SECTION

Synthesis. *General.* 5,5′-bis(5-Bromothiophen-2-yl)-4,4′-dihexyl-2,2′-bithiazole,[28] 2,5-bis(5-bromothiophen-2-yl)thiazolo[5,4-d]thiazole,[29−31] 6-bis(5-bromothiophen-2-yl)-1,2,4,5-tetrazine,[32] and 4,7-bis(5-bromothiophen-2-yl)-2,1,3-benzothiadiazole[33] were synthesized according to the procedure reported in the literature.

*4,9-Dihydro-4,4,9,9-tetradodecyl-indaceno[1,2-b:5,6-b′]-dithiophene (**2**)*[21]. To a suspension of compound **1** (2.66 g, 10.0 mmol) in anhydrous DMSO (50 mL) was added sodium *tert*-butoxide (7.68 g, 80.0 mmol) in parts. The reaction mixture was heated at 80 °C for 1 h, followed by addition of 1-bromododecane (13.4 g, 80.0 mmol) dropwise. After complete addition, the resultant mixture was heated at 90 °C for 8 h and then poured into ice−water. The precipitate was collected by filtration and washed with water and methanol to give a black solid. The solid was purified by column chromatography on silica, eluting with hexanes, to give an off-white solid (4.7 g, 50%). ^{1}H NMR (400 MHz, $CDCl_3$): δ (ppm) 7.29 (s, 2H), 7.27 (d, 2H), 6.98 (d, 2H), 1.94−2.04 (m, 4H), 1.81−1.92 (m, 4H), 1.02−1.46 (m, 76H), 0.75−0.98 (m, 24H).

*2,7-Dibromo-4,9-dihydro-4,4,9,9-tetradodecyl-indaceno[1,2-b:5,6-b′]-dithiophen (**3**).* To a solution of compound **2** (4.0 g, 4.25 mmol) in THF/DMF (2:1, 100 mL) was added *N*-bromosuccinimide (1.66 g, 9.35 mmol). This mixture was stirred for 3 h in the absence of light at room temperature and then poured into water. The precipitate was collected and washed with water and then recystallized with acetone, to give product as pale yellow solid (4.18 g, 90%).^{1}H NMR (400 MHz, $CDCl_3$): δ (ppm) 7.17 (s, 2H), 6.96 (s, 2H), 1.89−1.95 (m, 4H), 1.78−1.88 (m, 4H), 1.00−1.53 (m, 76H), 0.74−0.88(m, 24H).

*2,7-bis(Trimethyltin)-4,9-dihydro-4,4,9,9-tetradodecyl-s-indaceno-[1,2-b:5,6-b′]-dithiophene (**4**).* Compound **3** (4.37 g, 3 mmol) was dissolved in dry THF (100 mL). The solution was cooled to −78 °C, and butyllithium (2.5 M, 3 mL, 7.5 mmol) was added dropwise over 10 min. The reaction was stirred at this temperature for 1 h. Trimethyltin chloride (1 M in hexanes, 9.0 mL, 9.0 mmol) was added dropwise. The reaction was allowed to warm to room temperature and stirred overnight. Water was added, and the reaction was extracted with diethyl ether. The organic layer was washed with water and dried over magnesium sulfate. Evaporation of the solvent afforded the bis(trimethyltin) monomer as a light brownish viscous oil (4.5 g, 92%). ^{1}H NMR (400 MHz, $CDCl_3$): δ (ppm) 7.17 (s, 2H), 6.97 (s, 2H), 1.91−1.95 (m, 4H), 1.81−1.84 (m, 4H), 1.00−1.53 (m, 88H), 0.84−0.87(m, 30H). ^{13}C NMR (100 MHz, $CDCl_3$): δ (ppm) 158.0, 154.3, 148.5, 140.0, 136.1, 130.2, 114.3, 53.9, 40.0, 32.8, 30.9, 30.5, 30.5, 30.4, 30.2, 25.0, 23.6, 14.9, −7.2.

Synthesis of Copolymers. *Synthesis of **PIDT-BTz**.* 2,7-bis-(Trimethyltin)-4,9-dihydro-4,4,9,9-tetradodecyl-*s*-indaceno[1,2-*b*:5,6-*b*′]-dithiophene (633 mg, 0.5 mmol), 5,5′-bis(5-bromothiophen-2-yl)-4,4′-dihexyl-2,2′-bithiazole (329 mg, 0.5 mmol), and dry toluene (12 mL) were added to a 50 mL double-neck round-bottom flask. The reaction container was purged with argon for 20 min to remove O_2, and then Pd $(PPh_3)_4$ (15 mg) was added. After another flushing with argon for 20 min, the reactant was heated to reflux for 48 h. The reactant was cooled down to room temperature and poured into MeOH (200 mL) and then filtered through a Soxhlet thimble, which was then subjected to Soxhlet extraction with methanol, hexane, and chloroform. Polymer was recovered from the chloroform fraction by rotary evaporation as solid. The polymer was purified by chromatography on silica gel with chloroform as the eluent, and the polymer solution was concentrated and poured into MeOH. After this, the precipitates were collected and dried under vacuum overnight. Yield: 387 mg (54%). GPC: M_w = 24.9 K; M_n = 13.6 K; M_w/M_n = 1.83. ^{1}H NMR (400 MHz, $CDCl_3$), δ (ppm): 7.25 (s, 2H), 7.10−7.20 (m, 6H), 3.01(s, 4H), 1.85−2.0 (d, 12H), 1.2−1.4 (m, 76H), 0.83−0.93(m, 34H)

PIDT-TTz, **PIDT-TZ**, and **PIDT-DTBT** were synthesized according to the same procedure as **PIDT-BTz** with respective monomers. The ^{1}H NMR and gel permeation chromatography (GPC) data of the polymers are listed below.

PIDT-TTz. Yield: 385 mg (62%). M_w = 27.6 K; M_n = 17.4 K; M_w/M_n = 1.59. ^{1}H NMR (400 MHz, $CDCl_3$), δ (ppm): 7.51 (s, 2H), 7.18−7.28 (m, 6H), 1.9−2.0 (m, 8H), 1.14−1.20 (m, 72H), 0.84−0.97(m, 20H).

PIDT-TZ. Yield: 342 mg (58%). M_w = 13.3 K; M_n = 8.7 K; M_w/M_n = 1.64. ^{1}H NMR (400 MHz, $CDCl_3$), δ (ppm): 8.19 (s, 2H), 7.25−7.36 (m, 6H), 1.9−2.0 (d, 8H), 1.14−1.20 (m, 72H), 0.84−0.97(m, 20H).

PIDT-DTBT. Yield: 315 mg (51%). M_w = 21.3K; M_n = 11.7K; M_w/M_n = 1.82. ^{1}H NMR (400 MHz, $CDCl_3$), δ (ppm): 8.08 (s, 2H), 7.89 (s, 2H), 7.28(m, 6H), 1.9−2.0 (d, 8H), 1.14−1.20 (m, 72H), 0.84−0.97(m, 20H).

Measurements and Characterization. All new compounds were characterized by ^{1}H NMR spectroscopy performed on a Bruker DMX-400 spectrometer. For the ^{1}H NMR measurements, $CDCl_3$ was used as the solvent. Chemical shifts in the NMR spectra were reported in ppm relative to the singlet at 7.26 ppm for $CDCl_3$. The molecular weight of the polymers was measured by gel permeation chromatography (GPC), and polystyrene was used as a standard. Thermogravimetric analysis (TGA) was performed on a Perkin−Elmer TGA-7. Mass spectra were obtained with a Shimadzu QP2010 spectrometer. UV−vis absorption spectra were obtained on a Hitachi U-3010 spectrometer. Cyclic voltammetry (CV) was performed on a Zahner IM6e Electrochemical Workstation with a three-electrode system in a solution of 0.1 M Bu_4NPF_6 in acetonitrile at a scan rate of 100 mV/s. The polymer films were coated on a Pt plate electrode (1.0 cm^2) by dipping the electrode into the corresponding solutions and then drying. A Pt wire was used as the counter electrode, and Ag/Ag^+ was used as the reference electrode.

Device Fabrication and Characterization of Polymer Solar Cells. Polymer solar cells (PSCs) were fabricated with ITO glass as a positive electrode, Ca/Al as a negative electrode, and the blend film of the polymer/$PC_{70}BM$ between them as a photosensitive layer. The ITO glass was precleaned and modified by a thin layer of PEDOT:PSS which was spin-cast from a PEDOT:PSS aqueous solution (Clevious P VP AI 4083 H. C. Stark, Germany) on the ITO substrate, and the thickness of the PEDOT/PSS layer is about 60 nm. The photosensitive layer was prepared by spin-coating a blend solution of polymers and $PC_{70}BM$ in *o*-dichlorobenzene on the ITO/PEDOT:PSS electrode. Then, the Ca/Al cathode was deposited on the polymer layer by vacuum evaporation under 3×10^{-5} Pa. The thickness of the photosensitive layer is ca.100−120 nm, measured on an Ambios Tech. XP-2 profilometer. The effective area of one cell is 4 mm^2. The current−voltage (I−V) measurement of the devices was conducted on a computer-controlled Keithley 236 Source Measure Unit. A xenon lamp with AM1.5 filter was used as the white light source, and the optical power at the sample was 100 mW/cm^2.

dx.doi.org/10.1021/cm2019586 |*Chem. Mater.* 2011, 23, 4264–4270

AUTHOR INFORMATION

Corresponding Author
*E-mail: liyf@iccas.ac.cn.

ACKNOWLEDGMENT

This work was supported by NSFC (Nos. 20874106, 20821120293, 50933003 and 21021091), the Ministry of Science and Technology of China and the Chinese Academy of Sciences.

REFERENCES

(1) Yu, G.; Gao, J.; Hummelen, J. C.; Wudl, F.; Heeger, A. J. *Science* **1995**, *270*, 1789–1791.

(2) Liang, Y. Y.; Xu, Z.; Xia, J.; Tsai, S. T.; Wu, Y.; Li, G.; Ray, C.; Yu, L. P. *Adv. Mater.* **2010**, *22*, E135–E138.

(3) (a) Hou, J. H.; Chen, H. Y.; Zhang, S. Q.; Chen, R. I.; Yang, Y.; Wu, Y.; Li, G. *J. Am. Chem. Soc.* **2009**, *131*, 15586. (b) Chen, H.-Y.; Hou, J. H.; Zhang, S. Q.; Liang, Y. Y.; Yang, G. W.; Yang, Y.; Yu, L. P.; Wu, Y.; Li, G. *Nat. Photonics* **2009**, *3*, 649–653.

(4) (a) Chen, J. W.; Cao, Y. *Acc. Chem. Res.* **2009**, *42*, 1709–1718. (b) Wang, M.; Hu, X.; Liu, P.; Li, W.; Gong, X.; Huang, F.; Cao, Y. *J. Am. Chem. Soc.* **2011**, *133*, 9638–9641. (c) He, Z. C.; Zhang, C.; Xu, X. F.; Zhang, L. J.; Huang, L.; Chen, J. W.; Wu, H. B.; Cao, Y. *Adv. Mater.* **2011**, *23*, 3086–3089.

(5) (a) Thompson, B. C.; Fréchet, J. M. J. *Angew. Chem., Int. Ed.* **2008**, *47*, 58–77. (b) Li, Y. F.; Zou, Y. P. *Adv. Mater.* **2008**, *20*, 2952–2958. (c) Amb, C. M.; Chen, S.; Graham, K. R.; Subbiah, J.; Small, C. E.; So, F.; Reynolds, J. R. *J. Am. Chem. Soc.* **2011**, *133*, 10062–10065. (d) Su, M.-S.; Kuo, C.-Y.; Yuan, M.-C.; Jeng, U.-S.; Su, C.-J.; Wei, K.-H. *Adv. Mater.* **2011**, *23*, 3315–3319.

(6) Park, S. H.; Roy, A.; Beaupré, S.; Cho, S.; Coates, N.; Moon, J. S.; Moses, D.; Leclerc, M.; Lee, K. H.; Heeger, A. J. *Nat. Photonics* **2009**, *3*, 297–303.

(7) Chen, Y.-J.; Yang, S.-H.; Hsu, C.-S. *Chem. Rev.* **2009**, *109*, 5868–5923.

(8) (a) Wang, E. G.; Hou, L. T.; Wang, Z. Q.; Hellström, S.; Zhang, F. L.; Inganas, O.; Andersson, M. R. *Adv. Mater.* **2010**, *22*, 5240–5244. (b) Jiang, J.-M.; Yang, P.-A.; Chen, H.-C.; Wei, K.-H. *Chem. Commun* **2011**, *47*, 8877–8879.

(9) (a) Muhlbacher, D.; Scharber, M.; Morana, M.; Zhu, Z. G.; Waller, D.; Gaudiana, R.; Brabec, C. *Adv. Mater.* **2006**, *18*, 2884. (b) Svensson, M.; Zhang, F. L.; Veenstra, S. C.; Verhees, W. J. H.; Hummelen, J. C.; Kroon, J. M.; Inganas, O.; Andersson, M. R. *Adv. Mater.* **2003**, *15*, 988.

(10) (a) Zhang, Y.; Hau, S. K.; Yip, H.-L.; Sun, Y.; Acton, O.; Jen, A. K.-Y *Chem. Mater.* **2010**, *22*, 2696–2698. (b) Huang, F.; Chen, K.-S.; Yip, H.-L.; Hau, S. K.; Acton, O.; Zhang, Y.; Luo, J. D.; Jen, A. K.-Y. *J. Am. Chem. Soc.* **2009**, *131*, 13886–13887.

(11) (a) Blouin, N.; Michaud, A.; Leclerc, M. *Adv. Mater.* **2007**, *19*, 2295. (b) Blouin, N.; Michaud, A.; Gendron, D.; Wakim, S.; Blair, E.; Neagu-Plesu, R.; Belletete, M.; Durocher, G.; Tao, Y.; Leclerc, M. *J. Am. Chem. Soc.* **2008**, *130*, 732–742.

(12) Peet, J.; Kim, J. Y.; Coates, N. E.; Ma, W. L.; Moses, D.; Heeger, A. J.; Bazan, G. C. *Nat. Mater.* **2007**, *6*, 497–500.

(13) (a) Hou, J. H.; Chen, H. Y.; Zhang, S. Q.; Li, G.; Yang, Y. *J. Am. Chem. Soc.* **2008**, *130*, 16144. (b) Zhang, M. J.; Guo, X.; Li, Y. F. *Adv. Energy Mater.* **2011**, *1*, 557–560.

(14) Zhou, E. J.; Nakamura, M.; Nishizawa, T.; Zhang, Y.; Wei, Q. S.; Tajima, K.; Yang, C. H.; Hashimoto, K. *Macromolecules* **2008**, *41*, 8302–8305.

(15) (a) Zou, Y. P.; Najari, A.; Berrouard, P.; Beaupré, S.; Aïch, B. R.; Tao, Y.; Leclerc, M. *J. Am. Chem. Soc.* **2010**, *132*, 5330–5331. (b) Chu, T.; Lu, J.; Beaupr, S.; Zhang, Y.; Pouliot, J.; Wakim, S.; Zhou, J.; Leclerc, M.; Li, Z.; Ding, J.; Tao, Y. *J. Am. Chem. Soc.* **2011**, *133*, 4250–4253.

(16) (a) Zhou, H.; Yang, L.; Stuart, A.; Price, S.; Liu, S.; You, W. *Angew. Chem., Int. Ed.* **2011**, *50*, 2995–2998. (b) Price, S.; Stuart, A.; Yang, L.; Zhou, H.; You, W. *J. Am. Chem. Soc.* **2011**, *133*, 4625–4631.

(17) (a) He, Y. J.; Li, Y. F. *Phys. Chem. Chem. Phys.* **2011**, *13*, 1970–1983. (b) He, Y. J.; Chen, H.-Y.; Hou, J. H.; Li, Y. F. *J. Am. Chem. Soc.* **2010**, *132*, 1377–1382. (c) Zhao, G. J.; He, Y. J.; Li, Y. F. *Adv. Mater.* **2010**, *22*, 4355–4358. (d) He, Y. J.; Zhao, G. J.; Peng, B.; Li, Y. F. *Adv. Funct. Mater.* **2010**, *20*, 3383–3389. (e) Cheng, Y.-J.; Hsieh, C.-H.; He, Y. J.; Hsu, C.-H.; Li, Y. F. *J. Am. Chem. Soc.* **2010**, *132*, 17381–17383.

(18) (a) Roncali, J. *Chem. Rev.* **1997**, *97*, 173. (b) Scharber, M. C.; Wuhlbacher, D.; Koppe, M.; Denk, P.; Waldauf, C.; Heeger, A. J.; Brabec, C. L. *Adv. Mater.* **2006**, *18* (6), 789.

(19) (a) Chen, C.-P.; Chan, S.-H.; Chao, T.-C.; Ting, C.; Ko, B.-T. *J. Am. Chem. Soc.* **2008**, *130*, 12828. (b) Chen, Y.; Yu, C.; Fan, Y.; Hung, L.; Chen, C.; Ting, C. *Chem. Commun.* **2010**, *46*, 6503–6505. (c) Wu, J.-S.; Cheng, Y.-J.; Dubosc, M.; Hsieh, C.-H.; Chang, C.-Y.; Hsu, C.-S. *Chem. Commun.* **2010**, 3259.

(20) (a) Zhang, Y.; Zou, J.; Yip, H.-L.; Chen, K.-S.; Zeigler, D. F.; Sun, Y.; Jen, A. K. Y. *Chem. Mater.* **2011**, *23*, 2289–2291. (b) Zhang, Y.; Zou, J. Y.; Yip, H.-L.; Chen, K.-S.; Davies, J. A.; Sun, Y.; Jen, A. K.-Y. *Macromolecules* **2011**, *44*, 4752–4758.

(21) Zhang, W. M.; Smith, J.; Watkins, S. E.; Gysel, R.; McGehee, M.; Salleo, A.; Kirkpatrick, J.; Ashraf, S.; Anthopoulos, T.; Heeney, M.; McCulloch, I. *J. Am. Chem. Soc.* **2010**, *132*, 11437.

(22) Wong, K. T.; Chao, T.-C.; Chi, L.-C.; Chu, Y.-Y.; Balaiah, A.; Chiu, S.-F.; Liu, Y.-H.; Wang, Y. *Org. Lett.* **2006**, *8*, 5033.

(23) Li, Y. F.; Cao, Y.; Gao, J.; Wang, D. L.; Yu, G.; Heeger, A. J. *Synth. Met.* **1999**, *99*, 243–248.

(24) Hou, J. H.; Tan, Z. A.; Yan, Y.; He, Y. J.; Yang, C. H.; Li, Y. F. *J. Am. Chem. Soc.* **2006**, *128*, 4911.

(25) Scharber, M. C.; Mühlbacher, D.; Koppe, M.; Denk, P.; Waldauf, C.; Heeger, A. J.; Brabec, C. J. *Adv. Mater.* **2006**, *18*, 789.

(26) Malliaras, G. G.; Salem, J. R.; Brock, P. J.; Scott, C. *Phys. Rev. B* **1998**, *58*, 13411.

(27) Zheng, Q.; Jung, B. J.; Sun, J.; Katz, H. E. *J. Am. Chem. Soc.* **2010**, *132*, 5394.

(28) (a) Lee, J.; Jung, B. J.; Lee, S. K.; Lee, J. I.; Cho, H. J.; Shim, H. K. *J. Polym. Sci., Part A: Polym. Chem.* **2005**, *43*, 1845–1857. (b) Wong, W. Y.; Wang, X. Z.; He, Z.; Chan, K. K.; Djurisic, A. B.; Cheung, K. Y.; Yip, C. T.; Ng, A. M. C.; Xi, Y. Y.; Mak, C. S. K.; Chan, W. K. *J. Am. Chem. Soc.* **2007**, *129*, 14372–14380. (c) Li, K. C.; Huang, J. H.; Hsu, Y. C.; Huang, P. J.; Chu, C. W.; Lin, J. T.; Ho, K. C.; Wei, K. H.; Lin, H. C. *Macromolecules* **2009**, *42*, 3681–3693. (d) Zhang, M. J.; Fan, H. J.; Guo, X.; He, Y. J.; Zhang, Z. G.; Min, J.; Zhang, J.; Zhao, G. J.; Zhan, X. W.; Li, Y. F. *Macromolecules* **2010**, *43*, 5706–5712. (e) Zhang, M. J.; Fan, H. J.; Guo, X.; He, Y. J.; Zhang, Z. G.; Min, J.; Zhang, J.; Zhao, G. J.; Zhan, X. W.; Li, Y. F. *Macromolecules* **2010**, *43*, 8714–8717.

(29) Osaka, I.; Zhang, R.; Sauve, G.; Smilgies, D. M.; Kowalewski, T.; McCullough, R. D. *J. Am. Chem. Soc.* **2009**, *131*, 2521.

(30) Ando, S.; Nishida, J. I.; Tada, H.; Inoue, Y.; Tokito, S.; Yamashita, Y. *J. Am. Chem. Soc.* **2005**, *127*, 5336.

(31) (a) Shi, Q. Q.; Fan, H. J.; Liu, Y.; Hu, W. P.; Li, Y. F.; Zhan, X. W. *J. Phys. Chem. C* **2010**, *114*, 16843–16848. (b) Yang, M.; Peng, B.; Liu, B.; Zou, Y. P.; Zhou, K. C.; He, Y. H.; Pan, C. Y.; Li, Y. F. *J. Phys. Chem. C* **2010**, *114*, 17989–17994.

(32) Li, Z.; Ding, J. F.; Song, H. H.; Lu, J. P.; Tao, Y. *J. Am. Chem. Soc.* **2010**, *132*, 13160–13161.

(33) Hou, Q.; Xu, Y. S.; Yang, W.; Yuan, M.; Peng, J. B.; Cao, Y. *J. Mater. Chem.* **2002**, *12*, 2887.